Renewable Energy 36 (2011) 289–297

Contents lists available at ScienceDirect

Renewable Energy

journal homepage: www.elsevier.com/locate/renene

An analysis of beta type Stirling engine with rhombic drive mechanism

D.J. Shendage [a], S.B. Kedare [a], S.L. Bapat [b,*]

[a] Department of Energy Science and Engineering, Indian Institute of Technology Bombay, Powai, Mumbai 400 076, India
[b] Department of Mechanical Engineering, Indian Institute of Technology Bombay, Powai, Mumbai 400 076, India

ARTICLE INFO

Article history:
Received 27 October 2009
Accepted 28 June 2010
Available online 24 July 2010

Keywords:
Stirling engine
Rhombic drive
Overlapping volume

ABSTRACT

Stirling engine system is one of the options for electrifying a remote community not serviceable by the grid, which can operate on energy input in the form of heat. Major hurdle for the wide-spread usage of rhombic drive beta type Stirling engine is complexity of the drive and requirement of tight tolerances for its proper functioning. However, if the operating and geometrical constraints of the system are accounted for, different feasible design options can be identified. In the present work, various aspects that need to be considered at different decision making stages of the design and development of a Stirling engine are addressed. The proposed design methodology can generate and evaluate a range of possible design alternatives which can speed up the decision making process and also provide a clear understanding of the system design considerations. The present work is mainly about the design methodology for beta type Stirling engine and the optimization of phase angle, considering the effect of overlapping volume between compression and expansion spaces. It is also noticed that variation of compression space volume with phase angle remains sinusoidal for any phase difference. The aim of the present work is to find a feasible solution which should lead to a design of a single cylinder, beta type Stirling engine of 1.5 kW_e capacity for rural electrification.

© 2010 Elsevier Ltd. All rights reserved.

1. Introduction

Stirling engines are again becoming relevant due to shortage and high cost of fossil fuel. Stirling engines can run quietly on combustion of any fuel. These do not use valves and are generally compact and reliable, as combustion takes place outside the working space. Stirling engines also do not have the Ozone depletion potential. Stirling engines work on Stirling cycle and have high efficiency. The ideal Stirling cycle consists of two isothermal and two isochoric processes as depicted on P–V diagram in Fig. 1. The cycle operates between minimum and maximum temperatures, T_C and T_E. The limit on T_E is dependent on the material of construction for the system. The regenerator is a thermodynamic sponge, a porous mass of finely divided material and alternately accepts (process 4–1) and rejects (process 2–3) heat from working fluid as shown in Fig. 1.

Since Stirling engines are external heat source engines, they can also operate on concentrated solar energy and any gaseous or liquid fuels.

Thermal efficiency of Stirling engine is expected to be higher than that of Rankine cycle based systems. Stirling engine may also prove to be cheaper compared to solar photovoltaic units for 1.5 kW_e capacity. There are 96,000 villages in India to be electrified [1]. Of these more than 20,000 villages are in remote and difficult areas of the country, 3–30 km away from grid, with number of households below 200, average population less than 500, with time for power requirement quite low (of the order of 4–6 h/day) for minimal facilities. The grid connection for such villages is a very costly proposition and hence not easily taken up. Therefore, a Stirling engine with capacity of about 1.5 kWe seems to be the most viable option. It will, at least partially, help to overcome the present problem of scarcity of electrical energy in India, especially in remote regions. If biomass or agricultural waste is available as fuel many more applications may come up at small companies and communities [2].

Stirling engines of various configurations are developed over the years. Also different analysis methodologies are used for the purpose of analysis and comparison between systems. Shoureshi has compared Stirling, Rankine and Brayton engines at different practical temperature-ratios conditions and shows that Stirling engines are more efficient than others [3]. The "V"-type Stirling engines with sealed and dry crank-cases and fuelled by natural gas are presently under development at the Physical-Technical Institute and one of the major issues in improving kinematic Stirling engine performance was proper guiding of piston rings, while developing Radioisotope Stirling engines [4]. In other words, one has to design drive mechanism such that it should have minimum side thrust and

* Corresponding author. Fax: +91 22 25 72 68 75.
E-mail addresses: shendagedj@iitb.ac.in (D.J. Shendage), sbkedare@iitb.ac.in (S.B. Kedare), slbapat@iitb.ac.in (S.L. Bapat).

0960-1481/$ – see front matter © 2010 Elsevier Ltd. All rights reserved.
doi:10.1016/j.renene.2010.06.041

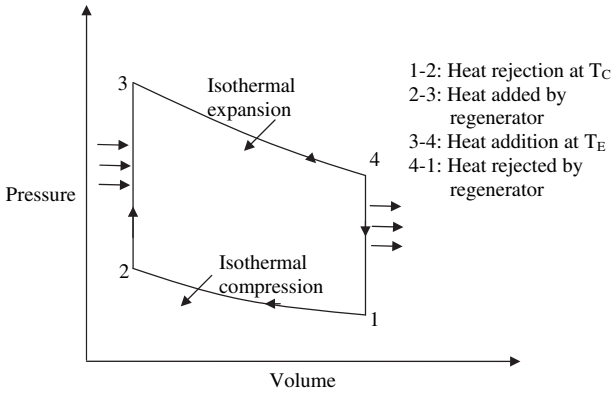

Fig. 1. Ideal Stirling cycle with complete regeneration.

jerky moment. The prime motivation for carrying out the present work was (i) to investigate the methodology for kinematic analysis, and (ii) to link kinematic analysis to the thermodynamic cyclic analysis, so that the mechanical phase angle, geometrical and operating parameters can be optimised. The paper addresses various aspects that need to be considered at different decision making stages of the design and development of Stirling engine. The rhombic drive mechanism chosen for the present work is analysed and designed in detail. The design methodology is proposed that will help in optimising Stirling engine. It is intended to exploit the advantage of overlapping volume to the fullest extent. The objective of the present work is to analyse the rhombic drive by considering different aspects which include

(1) selection of configuration of Stirling engine,
(2) design consideration in rhombic drive from assembly point of view, analysis of beta type engine with rhombic drive i.e. calculation of stroke, calculation of phase angle, selection of relative eccentricity ratio (ε), calculation of overlapped volume,
(3) mechanical design of rhombic drive by considering torque on crankshaft and buckling of piston rods and displacer rod and
(4) methodology to link the thermodynamic analysis and rhombic drive analysis with limitations and challenges in rhombic drive.

2. Selection of configuration of Stirling engine and drive mechanism

As shown in Fig. 2, three configurations, namely the alpha, beta and gamma configurations, are commonly used in Stirling engine [5]. Alpha configuration includes two pistons in separate cylinders

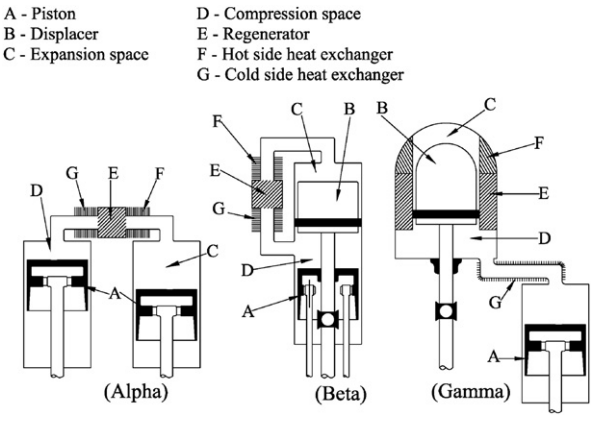

Fig. 2. Three basic mechanical configurations for Stirling engine.

and schematically has simple arrangement. In beta configuration, both displacer and cylinder are accommodated in same cylinder and has comparatively complex arrangement. Gamma configuration includes displacer and piston in separate cylinders and has simple arrangement. Though beta configuration is complex, it has merit over other types due to its ability to provide overlapping volume. The beta machine can have almost 30% larger heat exchangers than that for gamma machine for the same compression ratio [6]. In short, beta engine is selected due to its advantages like compactness, lower dead space involved and overlapping of volume.

The studies were carried out for different configurations, working fluid and heat sources. Miyabe et al. conducted various experiments on alpha type, Nitrogen charged, kinematic Stirling engine using crank mechanism with phase angle 90° and proposed design method for regenerator matrix [7]. Erich selected the α-type Stirling engine with crank mechanism due to cost reasons. Air or nitrogen as working fluid and many parts from industrial mass production had been used for development [2]. Biedermann et al. has developed 35 kW_e pilot plant with more than 5000 h of successful operation utilising wood chip fuels with overall electric efficiency 9.2% [8]. The engine uses, Helium as working fluid at 4.5 MPa mean pressure, the crank mechanism operating at 1010 rpm and has four cylinders and looking for improved reliability of driving mechanism. Thomas et al. have compared four Dish-Stirling systems, named as Sun Dish, Euro Dish, SES and WGA, which are developed for commercial applications [9]. The highest overall efficiency of the solar power generation system is nearly 30% and the issues for commercialising are cost and reliability [9,10]. TEDOM Company developed the functional prototype of kinematic Stirling engine, which has output of 7.9 kW at 1500 rpm with engine efficiency of 24.13% at 670 °C/50 °C temperatures at 11.2 MPa mean pressure of helium [11]. They observed that reliability of piston ring matters for long running of life and can be increased by proper design and selection of drive mechanism. Halit et al. analysed and tested a beta type Stirling engine with a lever controlled displacer driving mechanism, with pressurised crankcase kinematic and thermodynamics points of view [12–14]. The engine developed by Halit et al. is water cooled with helium charged and produces 183 W at 590 rpm [12]. It can be noticed that main challenges to develop reliable engine, are sealing of working fluid at high pressures and design of drive mechanism with minimum side thrust.

Can has analysed and developed a beta type Stirling engine using crank mechanism with air as working fluid at atmospheric pressure [15]. The same is cooled by water and has 90° phase angle and produces 5.98 W at 208 rpm with the hot-source temperature of 1000 °C. Youssef et al. have developed model considering thermodynamic analysis and can be useful to understand the influence of various geometrical and operating parameters for beta type Stirling engine [16]. Similarly, it is needed to develop methodology for the kinematic analysis of rhombic drive, which will consider effect of acceleration of links, and will able to couple with thermodynamic analysis. Hence, the designed engine will have long life with reliability. Mirunalini et al. have numerically analysed performance of a beta Stirling solar thermal engine system [17]. It can be observed that phase angle and regenerator volume plays vital role in engine performance [17,18]. But in beta type Stirling engine with rhombic drive mechanism, one can make use of overlapping volume in compression space and modify the mechanical phase angle for more power output with negligible sacrifice in efficiency.

It is clear from the above-reported studies that the requirement is of a reliable (with high reproducibility), long life engine with high specific power output and low fuel consumption presently. The drive mechanism has to be capable of providing the reciprocating

motion to both; the piston and the displacer; and simultaneously ensure the desired phase difference between their motions. There are three different considerations for selecting a suitable drive mechanism for a Stirling engine. The first is to choose a mechanism, which will carry the working gas through the cycle and provide the desired level of work output based on the heat input. The second consideration is mechanical efficiency, which means that the mechanism should have low frictional losses. The third consideration is the practical aspect such as the size, reliability and cost. Rhombic drive mechanism is chosen with clear expectation that all the three criteria as above will be satisfied. Beta engine with rhombic drive gives minimum side thrust, ensures silent working of engine. On analysis of the drive mechanisms viz., crank drive and rhombic drive, it was found that the rhombic drive mechanism gives a maximum power output 10% higher than the crank drive mechanism whereas its thermal efficiency is about 0.5% lower [19].

3. Beta type engine with rhombic drive

Rhombic drive was originally developed around 1900 for the twin-cylinder Lanchester car engine where it allowed perfect balancing of the inertial forces on both pistons [20]. The rhombic drive mechanism for Stirling engine was invented by Meijer of Philips, Holland in 1959 and used it extensively for beta type engines [19]. Fig. 3 shows the schematic diagram indicating the arrangement of components and the linkages used to provide reciprocating motion without side thrust for both, the piston (1) and the displacer (6). The two spur gears (10 and 10') mesh together and rotate in opposite directions as shown in Fig. 3. The whole arrangement is symmetric with respect to center line of the piston as well as the displacer. The two cranks (5 and 5') are of equal length *r*. Connecting rods (4 and 4') of equal length provide the link between the crank and the piston yoke (3). Piston rod (2) connects the piston yoke (3) with the piston (1) and thus provides the reciprocating motion to the piston (1). Similar to piston, the connecting rods (9 and 9') of equal length provide the link between the cranks (5 and 5') and the displacer yoke (8). If the two pairs of connecting rod i.e. 4, 4' and 9, 9' are made of identical lengths, they will form a rhombus. The name rhombic drive is for this reason.

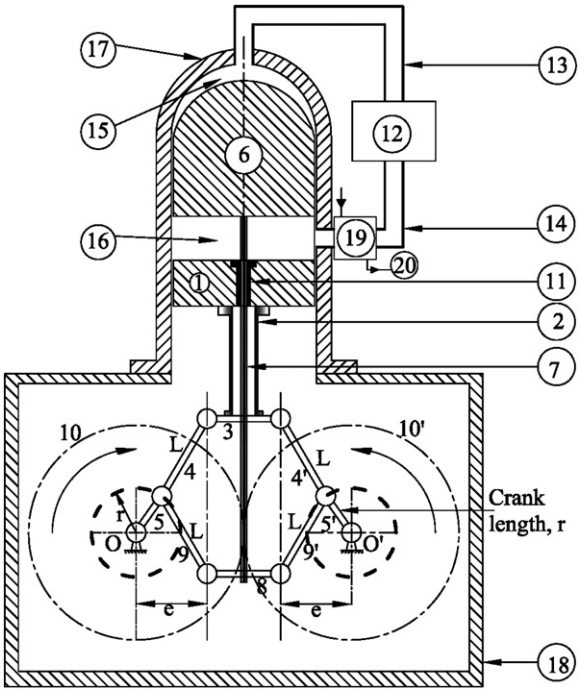

Fig. 3. Schematic of Stirling engine with the rhombic drive mechanism. 1: Piston; 2: Piston rod; 3: Piston yoke; 4, 4': Connecting rod (for piston yoke); 5, 5': Crank; 6: Displacer; 7: Displacer rod; 8: Displacer yoke; 9, 9': Connecting rod (for displacer yoke); 10, 10': Spur Gears; 11: Bush, 12: Regenerator, 13: Multiple heater tubes, 14: Connecting duct, 15: Expansion space, 16: Compression space, 17: Cylinder head, 18: Crankcase, 19: Cooler, 20: Coolant.

The displacer rod (7), connecting the displacer (6) to displacer yoke (8) has to pass through the piston 1 and also the compression space formed between the top surface of the piston and the bottom surface of displacer. It needs to be noted that the volume of compression space varies due to movement of not only the piston but also the displacer. However, the expansion space varies over a cycle only due to movement of the displacer. This movement of displacer rod through the piston needs a proper sealing arrangement as provided by bush (11). One of the shafts is generally used for cranking during 'start up' and the other shaft is used to provide energy output.

3.1. Design considerations in rhombic drive from assembly point of view

1) There are two ways of fixing the connecting rods on the crank pins shown in Fig. 4 as (a) Spilt connecting rod for piston yoke and (b) spilt connecting rod for displacer yoke [19]. The spilt connecting rod for piston arrangement has been chosen because of the following reason:
   (i) From assembly point of view, it is easy to assemble/disassemble.
   (ii) Gas forces on piston links will be higher than that of displacer. It will ensure safety from mechanical design point of view.
2) Arrangement of linking piston and piston yoke (upper arm) can be achieved by two methods (a) Piston and two solid piston rods arrangement and (b) Piston and annular piston rod arrangement. Arrangement with two solid piston rods (Fig. 5 (a)) is adopted. It serves following purposes:
   (i) Confirmation of piston in horizontal plane during assembly.
   (ii) It provides ease in piston seal assembly and inspection. Piston rods can be integral part of piston.
3) Alignment of crankshafts (Fig. 3) plays vital role in smooth and quiet running of the drive assembly. Gearwheels (10 and 10') ensure exact symmetry of the system at all times. The two crankshafts being geared together, the entire shaft output can be taken off from either of them. Although the gears are completely reliable, they tend to be subjectively noisy when compared to the overall quietness of the rest of Stirling engine. The gear noise can be reduced by reducing module of spur gear or using backlash free gearwheels.

3.2. Analysis and design considerations in rhombic drive

The special form of the rhombic drive mechanism is derived from the general form by excluding link between crank pin and

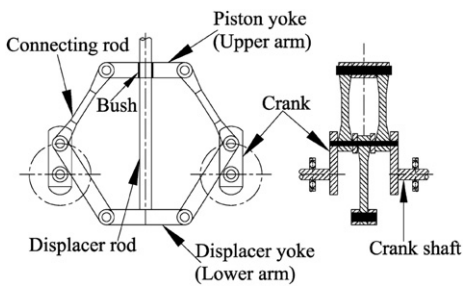

Fig. 4. Spilt connecting rod for piston yoke for rhombic drive mechanism.

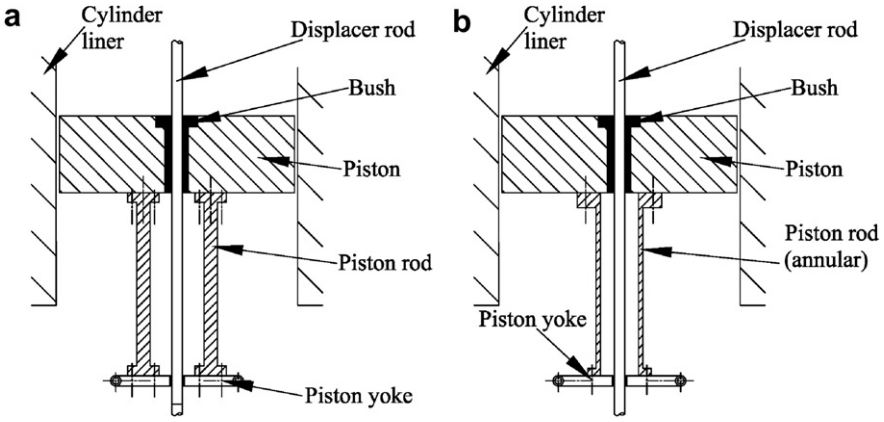

Fig. 5. (a) Piston and two piston rod arrangement (b) Piston and annular piston rod arrangement.

connecting rod and swivel joint, resulting in equal displacer and the piston strokes as shown in Fig. 6 [19]. Analysis of rhombic drive includes determination of stroke, phase angle and overlapping volumes for particular dimensions of crank length r, connecting rod length (L) and eccentricity (e).

3.2.1. Calculation of stroke

The stroke of the piston is equal to that of the displacer, because of the symmetry of the rhombic drive about y-axis as shown in Fig. 6. The displacer is in its lowest position when the displacer connecting rod and crank are in one straight line and its top position when displacer connecting rod covers the crank [19]. It follows that,

$$\frac{S}{r} = \frac{1}{\lambda}\left(\sqrt{(1+\lambda)^2-\lambda^2\varepsilon^2} - \sqrt{(1-\lambda)^2-\lambda^2\varepsilon^2}\right) \quad (1)$$

where,

$$\text{Eccentricity ratio} = \varepsilon = e/r \quad (\varepsilon > 1)$$

$$\text{and } \lambda = r/L \quad (e+r) < L$$

Thus, stroke can be calculated by using simple relation, having ε and λ as variables.

3.2.2. Calculation of phase angle

For the purpose of analysis, the cycle is combined to be split into a large number of equal intervals. The start of the cycle, for which the crank angle (Φ) should be 0° is the top most position of the displacer. Thus, at crank angle 0°, the expansion space volume is the minimum. Next, the value of crank angle when the piston will be in top most position is determined, knowing the various parameters. This will be the difference in motion between displacer and piston when the displacer leads the piston motion.

For ease of calculations (particularly for forces calculations) modified crank angle (ψ) is defined on basis of crank position for drive analysis. It is zero (0^0) when cranks are horizontal with inward position. Hence,

$$\text{Modified crank angle}(\Psi[i]) = \Phi[i] + \left(\begin{array}{l}\text{Angle difference between crank at}\\ \text{displacer TDC position and}\\ \text{horizontal position}\end{array}\right) \quad (2)$$

Meijer [19] has given numerical solution which uses series expansion of $\cos(n\psi)$. The sign convention for X is shown in Fig. 6. The abscissa of the displacer yoke is x_d and that of the piston yoke is x_p. Then, we have,

$$\frac{1}{\lambda}\cos\chi = \sum_{n=0}^{\infty} B_n \cos(n\psi) \quad (3)$$

where,

$\Psi = 0$, when both cranks are in same line and face each other, and

χ = angle which the piston connecting rod makes with x-axis as shown in Fig. 6.

The coefficient B_1 as function of λ and ε can be calculated [19]. Then, one can calculate, Phase angle $(\alpha) = 2\tan^{-1}(B_1)$.

3.2.3. Selection of relative eccentricity ratio (ε)

In present analysis relative eccentricity ratio (ε) is selected as 1.5 due to following reason:

As relative eccentricity ratio, ε increases, buckling force on connecting rod increases. This happens because the value of acceleration for the whole mechanism increases. Thus, though power output is increasing as relative eccentricity ratio increases, its value is to be restricted. Based on the data available for two manufactured units with rhombic drive (Table 1), we also considered eccentricity ratio only up to 1.5 in present work.

3.2.4. Calculation of overlapped volume

Overlap volume is the volume of cylinder which is used both by the movement of the displacer and the piston as shown in Fig. 7 (a).

Modeling the expansion space height H_{exp}, from Fig. 7 (b) we get,

$$H_{exp} = (h_e - h_c) - r\cdot\sin\alpha_1 + L\cdot\sin\beta_1 \quad (4)$$

Similarly, for compression space height H_{comp}

$$H_{comp} = (h_c - h_2 - h_1) - 2L\cdot\sin\beta_1 \quad (5)$$

Also, from geometrical constraints,

$$e = r\cdot\cos\alpha_1 + L\cdot\cos\beta_1 = \text{constant} \quad (6)$$

Now, using the fact that,

Minimum$\{H_{exp}\}$ = Minimum$\{H_{comp}\}$ = 0, and using above three equations, eliminating constants [22], we finally get,

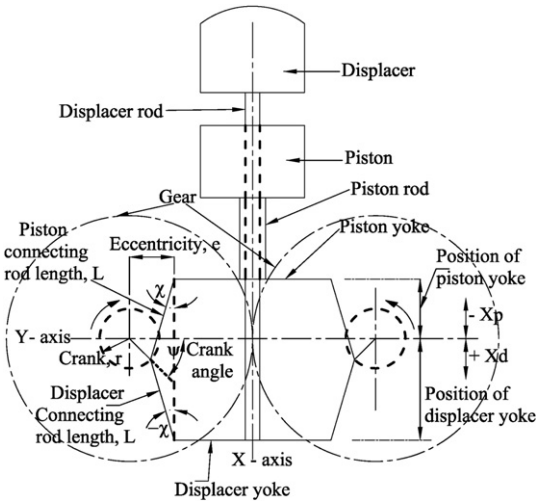

Fig. 6. Special form of rhombic drive obtained from general form [19].

$$H_{\text{exp}} = -(L-r)\sqrt{1-\left(\frac{e}{L-r}\right)^2} - r\cdot\sin\alpha_1 + L\cdot\sin\beta_1 \tag{7}$$

and,

$$H_{\text{comp}} = 2L\left[\sqrt{1-\left(\frac{e-r}{L}\right)^2} - \sin\beta_1\right] \tag{8}$$

The overlap length, as can be seen from Fig. 7(a and b), can be written as,

$$\begin{aligned}\text{OH}_{\max} &= \text{Maximum}\{H_{\text{exp}} + h_1\} \\ &\quad - \text{Minimum}\{H_{\text{exp}} + H_{\text{comp}} + h_1\}\end{aligned}$$

$$\text{OH}_{\max} = 2\left\{\sqrt{(r+L)^2 - e^2} - \sqrt{L^2 - (e-r)^2}\right\} \tag{9}$$

where, $\text{OH}_{\max}$ = Maximum overlapping height

which is again obtained by using previous equation. Values of r, L and e have to be chosen such that we get maximum possible overlap ensuring that the cylinder volume is properly utilised.

It is observed that for particular value of set of phase angle (78.5°), maximum overlapping stroke is 0.596 times stroke. During operations some wear is expected. This can cause a play in bushes at crankshafts, crank pins, connecting rods, displacer yoke and piston yoke. To account for these, clearance is provided in between piston and displacer. This clearance is calculated using the following relationship.

$$\text{CL}_{\min} = \left[0.005x\frac{S}{1000} + 0.5\right]/1000 \tag{10}$$

Table 1
Major dimensional data for the rhombic drive for the two engines (Mean pressures are different for engines).

	30 kW, Beta type, Meijer's engine [19]	3 kW, GPU-3 Engine [21]
$r \times 10^2$ (m)	2.65	1.397
$e \times 10^2$ (m)	3.92	2.065
$L \times 10^2$ (m)	8.8	4.602
e/r	1.4792	1.478
L/r	3.32	3.294

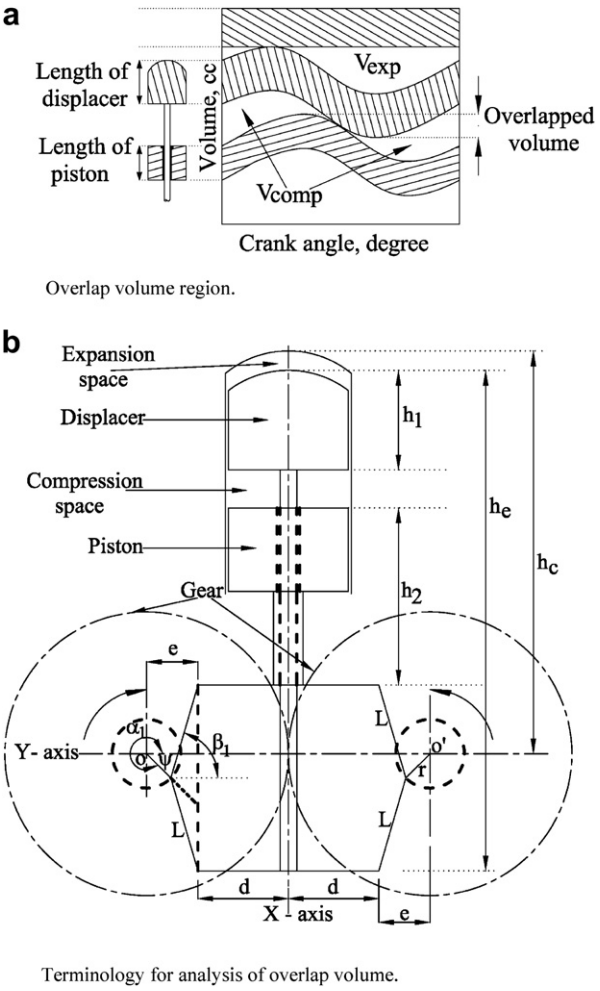

Fig. 7. (a) Overlap volume region. (b) Terminology for analysis of overlap volume.

Considering above aspect, maximum overlapping height is restricted only to 0.55 times of stroke for further analysis.

$$\text{i.e. } \frac{\text{OH}_{\max}}{S} \approx 0.55 \tag{11}$$

For further analysis, overlapping volume and clearance volume can be evaluated as follows,

$$V_{\text{dis}_{\text{cle}}} = \frac{\pi}{4}(d_{\text{dis}})^2 * \text{CL}_{\min} \tag{12}$$

$$V_{\text{pis}_{\text{cle}}} = \frac{\pi}{4}(d_{\text{pis}} - d_{\text{disrod}}) * \text{CL}_{\min} \tag{13}$$

$$V_{\text{pis}_{\text{OVERLAPPING}}} = \frac{\pi}{4}\left(d_{\text{pis}}^2 - d_{\text{disrod}}^2\right) * (\text{Overlapping length}) \tag{14}$$

where,

$V_{\text{dis}_{\text{cle}}}$ = Displacer clearance volume

$V_{\text{pis}_{\text{OVERLAPPING}}}$ = Overlapping volume

3.3. Mechanical design of rhombic drive

In the present case, the stroke of piston is equal to that of the displacer, because of the symmetry of the rhombic drive about the vertical axis. The displacer is in its lowest position (BDC) when the displacer connecting rod forms a continuation of the crank. And

it is at top position (TDC) when the displacer connecting rod covers (coincides with) the crank. For analysis and mechanical design of Rhombic drive first step to follow is to determine stroke (S), angle with vertical axis (X) at various crank angle (Φ) with use of Eqs. (1) and (2). Then, calculate torque on crankshafts due to the gas forces and inertia forces as discussed below.

3.3.1. Calculation of torque on crankshaft

The calculation of the torque is based on the energy balance of the engine. The rhombic drive is symmetrical at any instant during operation. It is assumed that the drive is completely balanced. Hence, half of the rhombic drive mechanism is considered for analysis. Various forces and moments occurring in the rhombic drive mechanism are shown in Fig. 8. Resultant torque on crankshaft is summation of torque due to gas forces, inertia forces and friction, and is evaluated as:

$$\underbrace{T_t}_{\text{Resultant torque}} = \underbrace{\frac{1}{2}F_p\frac{\dot{x}_p}{\omega}+\frac{1}{2}F_d\frac{\dot{x}_d}{\omega}}_{\text{Torque due to gas forces of circuit and crankcase}} - \underbrace{\frac{P_f}{\omega}}_{\text{Torque due to friction}} - \underbrace{\frac{d\sum E}{d\psi}}_{\text{Torque due to inertia forces}} \tag{15}$$

Different torques considered to calculate resultant torque are as follows:

1. Torque due to gas forces on piston: It is resultant of forces due to working space pressure and buffer/crankcase pressure acting on the piston itself and crankcase pressure acting on piston rod.
2. Torque due to gas forces on displacer: The gas force on the displacer is due to the pressure difference between the expansion space and compression space, which is caused by flow resistance in heat exchangers and by the force on displacer rod caused by pressure in the working space and in crankcase.
3. Torque due to inertia forces: It depends on speed and masses of rotating gearwheels and reciprocating components in engine assembly. Data is generated for calculating masses of components.
4. Torque due to friction: It requires knowledge of the coefficient of friction of piston and bearings, which is largely lacking since these variables depend on a large number of factors. From experience of IC Engines, generally torque due to friction is not major share on crankshaft. However, the total power of a well built Stirling engine is only about 10% of the power delivered by the engine [19]. In present work, frictional power in drive mechanism and engine subassemblies is considered as 15% of power developed by the engine.

The formulae given below are used in programming to calculate forces on different linkages. It is assumed that connecting rods are replaced by weightless rods and with certain masses at ends having certain moments of inertia [19]. However, calculation of torque due to inertia forces does not give actual force distribution along connecting rods but a mean value, which is sufficient for the strength calculations. For analysis the forces on the piston drive mechanism for the ith interval are,

$$F_{p1}[i] = \frac{1}{2}\left(F_p[i] - m_p\ddot{x}^i_{pis}\right) \tag{16}$$

$$F_{p2}[i] = \frac{1}{2}\left(F_p[i] - m_o\ddot{x}^i_{pis}\right)\tan\chi \tag{17}$$

$$F_{p3}[i] = \frac{1}{2}\left(F_p[i] - m_o\ddot{x}^i_{pis}\right)\sec\chi \tag{18}$$

$$F_{p4}[i] = 0 \tag{19}$$

$$F_{p5}[i] = F_{p3}[i]\sin(\chi[i]-\psi[i]) - m_{pc}\left(1-\frac{a_{pc}}{L}\right)r\omega^2 \tag{20}$$

$$F_p[i] = F_{p3}[i]\cos(\chi[i]-\psi[i]) \tag{21}$$

Similarly, forces on displacer drive linkages for ith interval are:

$$F_{d1}[i] = -\frac{1}{2}\left(F_d[i] - m_d\ddot{x}^i_{dis}\right) \tag{22}$$

$$F_{d2}[i] = -\frac{1}{2}\left(F_d[i] - m_o\ddot{x}^i_{dis}\right)\tan\chi \tag{23}$$

$$F_{d3}[i] = -\frac{1}{2}\left(F_d[i] - m_o\ddot{x}^i_{dis}\right)\sec\chi \tag{24}$$

$$F_{d4}[i] = 0 \tag{25}$$

$$F_{d5}[i] = F_{d3}[i]\sin(\chi[i]+\psi[i]) - m_{dc}\left(1-\frac{a_{dc}}{L}\right)r\omega^2 \tag{26}$$

$$F_{d6}[i] = F_{d3}[i]\cos(\chi[i]+\psi[i]) \tag{27}$$

$$F_7[i] = F_{p3}[i]\sin(\chi[i]-\psi[i]) + F_{d3}[i]\sin(\chi[i]+\psi[i]) + m_o r\omega^2 \tag{28}$$

$$F_8[i] = F_{p3}[i]\cos(\chi[i]-\psi[i]) - F_{d3}[i]\cos(\chi[i]+\psi[i]) \tag{29}$$

$$\dot{x}^{i+1}_{pis} = \left[\frac{sd^{i+2}_{pis}+sd^{i+1}_{pis}}{2} - \frac{sd^{i+1}_{pis}+sd^{i}_{pis}}{2}\right] \Big/ (\text{Interval time}) \tag{30}$$

$$\dot{x}^{i+1}_{dis} = \left[\frac{sd^{i+2}_{dis}+sd^{i+1}_{dis}}{2} - \frac{sd^{i+1}_{dis}+sd^{i}_{dis}}{2}\right] \Big/ (\text{Interval time}) \tag{31}$$

$$\ddot{x}^{i+1}_{pis} = \left[\dot{x}^{i+1}_{pis} - \dot{x}^{i}_{pis}\right] \Big/ (\text{Interval time}) \tag{32}$$

$$\ddot{x}^{i+1}_{dis} = \left[\dot{x}^{i+1}_{dis} - \dot{x}^{i}_{dis}\right] \Big/ (\text{Interval time}) \tag{33}$$

$$F_d[i] = \frac{\pi}{4}d^2_{dis}P_{exp}[i] - \frac{\pi}{4}\left(d^2_{dis}-d^2_{disrod}\right)P_{comp}[i] - \frac{\pi}{4}\left(d^2_{disrod}\right)P_{avg} \tag{34}$$

$$F_p[i] = \frac{\pi}{4}\left(d^2_{pis}-d^2_{disrod}\right)P_{comp}[i] - \frac{\pi}{4}\left(d^2_{pis}-d^2_{disrod}\right)P_{avg} \tag{35}$$

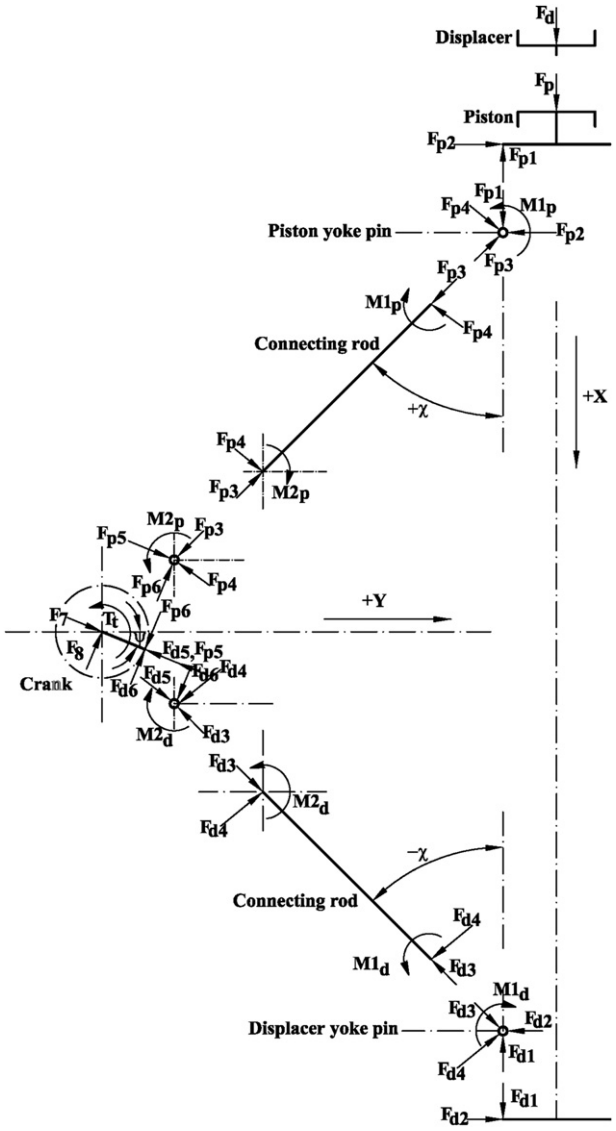

Fig. 8. Various forces and moments occurring in the rhombic drive mechanism [19].

$T_t[i]$ is torque on crankshaft at particular crank angle, can be calculated using above equations. Average torque throughout interval $T_{t_{avg}}[i]$ can be calculated as,

$$T_{t_{avg}}[i] = \frac{T_t[i+1] + T_t[i]}{2} \tag{36}$$

Energy output throughout interval $E[i]$ can be calculated as,

$$E[i] = T_{t_{avg}}[i]^* d\psi \tag{37}$$

Mean torque $(T_{t_{mean}})$ throughout the cycle can be calculated as,

$$T_{t_{mean}} = \frac{\sum E[i]}{\sum d\psi} \tag{38}$$

By using $T_{t_{avg}}[i]$ variation of torque with crank angle is plotted. This is known as turning moment diagram. From graph maximum energy point and minimum energy point can be calculated by using Eq. (39). Hence, flywheel can be designed by considering two different basis: i) on basis of energy released, coefficient of fluctuations (C_f), mass moment of inertia, density of gear material, module and pitch circle diameter of gear. ii) on basis of starting torque to ensure sufficient strength.

$$U_O = (E_{max}) - (E_{min}) \tag{39}$$

3.3.2. Design for buckling of piston rods and displacer rod

In present work, two piston rods are provided. Hence, the critical load will be shared by both piston rods equally. The maximum force on piston $F_p[i]$ is calculated for particular set of operating conditions. Assuming factor of safety, length of rod and diameter of rod is calculated using Johnson and Euler's theory for buckling of rod [23]. Simultaneously this procedure is extended for displacer rod by using maximum force on displacer rod for same set of operating conditions.

3.4. Methodology to link the thermodynamic analysis and rhombic drive analysis

1. The procedure takes into account all constraints discussed above. Initially, by using Beale number, average pressure and using bore to stroke ratio, stroke length is calculated. Eccentricity ratio (ε) is iterated such that it satisfies $\lambda < 1.5$ to calculate prescribed stroke.
2. One cycle of operation is divided into large intervals. For each interval compression space height (H_{comp}) and expansion space height (H_{exp}) is calculated. It is also ensured that mechanism operates within the geometrical constraints.
3. Overlapping volume, compression space and expansion space live volumes are calculated for each interval. These volumes are input for cyclic analysis of Stirling engine.
4. Piston and displacer velocities are calculated using displacement of respective links and interval time for a given speed i.e. 1440 rpm. It makes possible to use generator on same shaft of the engine.
5. Then, phase angle of engine is optimised on basis of maximum net brake power of engine.
6. Various forces and moments occurring in the rhombic drive mechanism are calculated by using energy balance and link velocities. Resultant torque is summation of all torques on crankshaft.

3.5. Limitations and challenges in rhombic drive

Usage of rhombic drive Beta type Stirling engine is presently quite restricted due to the drive's complexity and requirement of tight tolerances for its proper functioning. If during the operation there is an unsymmetrical wear of the pins or joints of the drive arrangement then it could lead to severe damage to the engine [6,24]. It involves large no. of moving parts in the assembly, which could again lead to wear and tear of various rubbing parts.

Some demerits of Beta engine which can be overcome by advancement of technology are discussed below.

a) These designs are complex to construct as to fit both the displacer and the piston in one cylinder. And it requires a high quality of precision fit to be done.
b) Piston seal leakage depends on clearance between piston bush and displacer rod. And it is difficult task to maintain appropriate clearance in running condition for long time as both are continuously moving. Hence, alignment during drive assembly should be done with almost care. Use of different fixtures will help a lot.
c) Major reason for vibrations during operation is jerky motion of links. It can be controlled by suitably selecting crank radius, eccentricity and length of connecting rod dimensions. From table provided for different eccentricity ratio (B_1) values by Meijer [19], it is observed that B_1 should be less than 1.5 to avoid jerking motion.

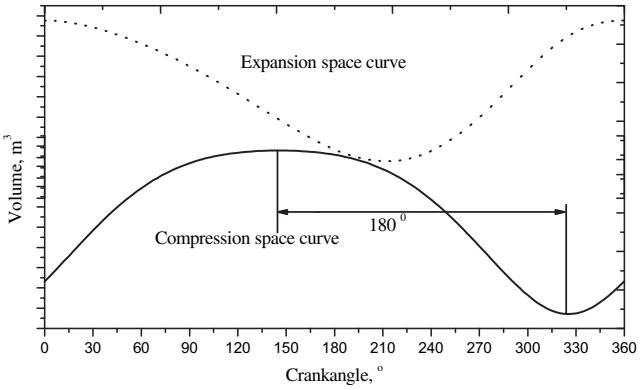

Fig. 9. Expansion and compression volume variations.

d) Backlash in gear and bearing clearance creates vibrations in machine. But in present case forces on teeth at running condition are at same direction. Engine operation depends on smooth operation of drive and gear assembly.

4. Results and discussion

i) On analysis of the drive mechanisms viz., crank drive and rhombic drive, it was found that the rhombic drive mechanism gives a maximum power output 10% higher than the crank drive mechanism whereas its thermal efficiency is about 0.5% lower.

ii) Fig. 9 shows volume variation of non-sinusoidal motion with respect to crank angle. At crank angle equal to zero, displacer is at TDC position and we will get maximum compression space volume at particular instant. As shown in Fig. 9, maximum average pressure intervals and overall time achieved for expansion is more by this configuration. Expansion takes place from 0° to 212.5° crank angle (i.e. approximately 60% of total cycle interval). Hence power output increases. Fig. 10 shows stroke (S) variation of non-sinusoidal motion with respect to crank angle. Theoretically, maximum overlapping stroke can be achieved is 0.596 times the stroke of displacer or piston.

iii) It is also noticed that compression space volume curve remains sinusoidal for any phase difference. To increase displacer dwelling period at compression piston and increase in overlapping volume one can think of shifting of compression curve towards left. But it is not recommended because indirectly length of connecting rod has to increase and acceleration of links will increase. It will cause buckling of connecting rods and its intensity will be higher due to cyclic stresses.

iv) Fig. 11 shows torque variation due to gas forces and mass inertia forces for 1500 W_e engine at designed conditions.

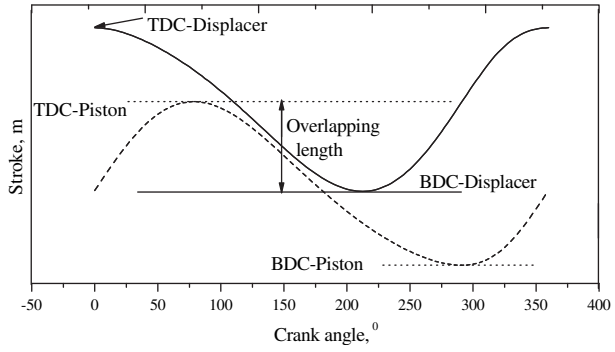

Fig. 10. Stroke variations of piston and displacer.

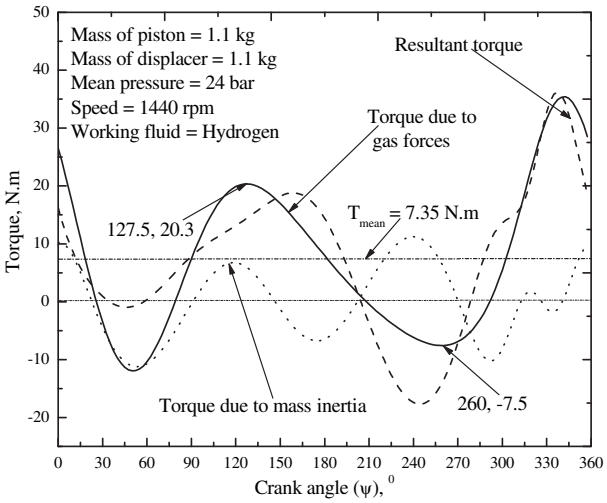

Fig. 11. The torque due to gas forces (working spaces) and torque due to the inertia (constant angular velocity) on one crankshaft at 24 bar mean pressure.

It can be seen from Fig. 11 that torque due to gas forces has major contribution in resultant torque.

5. Conclusions

In the present work, rhombic drive mechanism for Stirling engine application is analysed. The present work is mainly about the design procedure for beta type Stirling engine and the optimization of phase angle, considering the effect of overlapping volume between compression and expansion spaces. Methodology to link the thermodynamic analysis and rhombic drive analysis is also reported. Major conclusions from the present work are listed below:

1. As eccentricity ratio increases, it will enhance the power output. Simultaneously, it will demand for increase in connecting rod length. Then, buckling problem will become predominant. It will result into an unsymmetrical wear of the pins or joints of the drive arrangement during the operation. Then, it could lead to severe damage to the engine. Hence, eccentricity ratio for rhombic drive mechanism is fixed as 1.5.
2. It is also noticed that variation of compression space volume with phase angle remains sinusoidal for any phase difference. It improves power output (by around 10%) compared to crank driven beta Stirling engine for same geometrical and operating parameters.
3. It discusses about various aspects to be considered in rhombic drive by assembly point of view e.g. assembly of connecting rods and piston rods.
4. The effect of displacer and piston mass, connecting rods and yokes is considered along with pressure forces in working spaces for plotting the turning moment diagram. It also gives basis for flywheel design.
5. Present work gives design methodology for beta type Stirling engine and optimization of phase angle considering effect of overlapping volume.
6. The proposed design methodology can generate and evaluate a range of possible design alternatives which can speed up the decision making process and also provide a clear understanding of the system design considerations. The aim of the present work is to find a feasible solution which should lead to a design of a single cylinder, beta type Stirling engine of 1.5 kW_e capacity for rural electrification.

Acknowledgement

The authors acknowledge the financial support from Ministry of New and Renewable Energy, Government of India, to carry out the present work.

Nomenclature

a_{dc}: Distance from center of big end connecting rod of displacer and center of gravity of displacer connecting rod, m
a_{pc}: Distance from center of big end connecting rod of piston and center of gravity of displacer connecting rod, m
B_1: Expansion series coefficient (constant)
C_f: Coefficient of fluctuations
CL_{min}: Minimum clearance, m
C_s: Starting coefficient
d_{dis}: Diameter of displacer, m
d_{disrod}: Diameter of displacer rod, m
d_{pis}: Diameter of the piston, m
e: Eccentricity in rhombic drive mechanism, m
E: Kinetic energy of half of the rhombic drive, J
F: Gas force, N
H_{comp}: Compression space height, m
H_{exp}: Expansion space height, m
i: Interval
I_m: Mass moment of inertia, kg.m^2
L: Length of connecting rod for piston/displacer, m
m: Module of gear, m
m_{co}: Mass of counterweight, kg
m_{cr}: Mass of crankshaft, kg
m_d: Mass of displacer, displacer rod and displacer yoke together, kg
m_{dc}: Mass of displacer connecting rod, kg
m_p: Mass of piston, piston rod and piston yoke together, kg
m_{pc}: Mass of piston connecting rod, kg
N: Speed, rpm
OH_{max}: Maximum overlapping height, m
P: Pressure in engine at particular interval, bar
P_{max}: Maximum pressure in the working space, bar
P_{min}: Minimum pressure in the working space, bar
PCD: Pitch circle diameter of gear, m
P_f: Total power consumed by friction of the drive mechanism, W
r: Crank radius of rhombic drive, m
r_c: Volume ratio developed by the compressor (maximum volume/minimum volume)
S: Stroke, m
Sd_{dis}: Stroke of displacer, m
Sd_{pis}: Stroke of piston, m
T_C: Compression space temperature, K
T_E: Expansion space temperature, K
T_t: Resultant torque on crankshaft, N m
$T_{t_{mean}}$: Mean torque over the cycle, N m
U_o: Kinetic energy, J
V: Volume, m^3
V_{Comp}: Instantaneous compression space volume, m^3
$V_{dis_{cle}}$: Displacer Clearance volume (dead), m^3
V_{Exp}: Instantaneous expansion space volume for expansion space, m^3
$V_{pis_{overlapping}}$: Overlapping volume, m^3
x_d: Instantaneous position of the displacer, m
x_p: Instantaneous position of the piston, m
$\dot{x}$: Velocity, m/s
$\ddot{x}$: Acceleration, m/s^2
ρ_g: Density of gear material, kg/m^3
λ: Ratio of crank radius to the length of connecting rod, r/L
ψ: Modified crank angle, radian
ε: Eccentricity ratio, e/r
Φ: Crank angle, radian
χ: Angle which the piston connecting rod makes with X-axis, radian
ω: Angular velocity, rad/sec
β_1: Angle which the piston connecting rod makes with X-axis, radian
α_1: Angle which the crank makes with Y-axis, radian

Subscripts
avg: Average
cle: Clearance
comp: Compression space
d, dis: Displacer
exp: Expansion Space
max: Maximum
min: Minimum
p, pis: Piston

References

[1] Sastry EVR. "Village electrification programme in India", 3rd World Conference on Photovoltaic Energy Conversion, Osaka, Japan, May 11–18, 2003.
[2] Erich P. Electricity production in rural villages with a biomass Stirling engine. Renewable Energy 1999;16:1049–52.
[3] Shoureshi R. Analysis and design of Stirling engines for waste-heat recovery, Ph.D. thesis, M.I.T., 1981.
[4] Makhkamov K, et al. Development of solar and micro co-generation power installations on the basis of Stirling engines, AIAA-2000-2931, pp 723–733.
[5] Walker G. Stirling engine. New York: Oxford University Press; 1980.
[6] West CD. Principles and applications of Stirling engines. 15-63. New York: Van Nostrand Reinhold Company; 1986.
[7] Miyabe H, Takahashi S, Hamaguchi K. An approach to the design of Stirling engine regenerator matrix using packs of wire gauzes, Proc. 17th IECEC, pp.1839–1844, 1982.
[8] Biedermann F, Carlsen H, Schoech M, Obernberger I. Operating experiences with a small-scale CHP pilot plant based on a 35 kWel hermetic four cylinder Stirling engine for Biomass fuels, The 11th International Stirling Engine Conference, Rome, November 19–21, 2003.
[9] Thomas M. Dish-Stirling systems: an overview of development and status. Journal of Solar Energy Engineering, Trans. ASME 2003;125:135–51.
[10] Sukhatme SP, Nayak JK. Solar energy principles of thermal collection and storage. New Delhi: Tata McGraw Hill Co.; 2007.
[11] http://engine.stirling.cz/tedom-stirling-engine.html, website assessed on 10/05/2008.
[12] Karabulut H, Cinar C, Ozturk E, Yucesu H. Torque and power characteristics of a helium charged Stirling engine with a lever controlled displacer driving mechanism. Renewable Energy 2010;35:138–43.
[13] Halit K, Huseyin SY, Can C, Fatih A. An experimental study on the development of a β-type Stirling engine for low and moderate temperature heat sources. Applied Energy 2009;86:68–73.
[14] Halit K, Fatih A, Erkan O. Thermodynamic analysis of a β type Stirling engine with a displacer driving mechanism by means of a lever. Renewable Energy 2009;34:202–8.
[15] Can C, Serdar Y, Tolga T, Melih O. Beta-type Stirling engine operating at atmospheric pressure. Applied Energy 2005;81:351–7.
[16] Youssef T, Iskander T, Sassi BN. Technical note: performance optimization of Stirling engines. Renewable Energy 2008;33:2134–44.
[17] Thirugnanasambandam M, Iniyan S, Goic R. A review of solar thermal technologies. Renewable and Sustainable Energy Reviews 2010;14:312–22.
[18] Kerdchang P, Win M, Teekasap S, Hirunlabh J, Khedari J, Zeghmati B. Development of a new solar thermal engine system for circulating water for aeration. Solar Energy 2005;78:518–27.
[19] Meijer RJ. The Philips Stirling Thermal Engine, analysis of the rhombic drive mechanism and efficiency measurements, Thesis, Technical University, Delft, Nov. 1960.
[20] http://en.wikipedia.org/wiki/Rhombic_drive#History, website assessed on 26/02/2010.
[21] Martini W. Stirling engine design manual. NASA Report; 1978.
[22] http://mac6.ma.psu.edu/stirling/drives/index.html, website assessed on 05/03/2006.
[23] Shigley JE. Mechanical engineering design. Mechanical engineering series. McGraw-Hill publication; 1986.
[24] Shendage DJ, Kedare SB, Bapat SL. "Design and development of Stirling engine", Papyrus – Book of Papers, Energy Day 2009, Department of Energy Science and Engineering, Indian Institute of Technology, Bombay on March 21, 2009 (Technical session IA), pp 10–12.